Landerer, F. W., Dickey, J. O., Güntner, A. (2010): Terrestrial water budget of the Eurasian pan-Arctic from GRACE satellite measurements during 2003 - 2009. - Journal of Geophysical Research, 115, D23115

DOI: 10.1029/2010JD014584

Terrestrial water budget of the Eurasian pan-Arctic from GRACE satellite measurements during 2003–2009

Felix W. Landerer,[1] Jean O. Dickey,[1] and Andreas Güntner[2]

Received 4 June 2010; revised 29 August 2010; accepted 16 September 2010; published 4 December 2010.

[1] We assess the controls of the terrestrial water budget over the Eurasian pan-Arctic drainage region from 2003 to 2009 by combining observations from the Gravity Recovery and Climate Experiment (GRACE) with reanalysis estimates of net precipitation and observations of river discharge from gauges. Of particular interest are the expansive permafrost regions. Thawing permafrost has been implicated to contribute to the observed discharge increases through the melting of excess ground ice. We show that terrestrial water storage (TWS) over large areas of the Eurasian pan-Arctic region has increased during 2003–2009. However, significant interannual TWS variability is present and most TWS increases occur over nonpermafrost regions in the Ob and Yenisei basins. Over the central Lena basin, which is mostly underlain by permafrost, TWS steadily increased until 2007 but has slightly declined since. By combining GRACE observations of TWS anomalies with discharge and net precipitation, we show that the terrestrial water budget is at least qualitatively closed over the Eurasian Arctic basins. The observed TWS and discharge increases over the study time period were driven by increased atmospheric moisture fluxes. Therefore, we conclude that melting of excess ground ice in permafrost regions did not act as a source to observed changes in discharge. Nonetheless, the signature of significant TWS increases points to ongoing thickening of the active layer in particular over the discontinuous permafrost regions in the central Lena basin.

Citation: Landerer, F. W., J. O. Dickey, and A. Güntner (2010), Terrestrial water budget of the Eurasian pan-Arctic from GRACE satellite measurements during 2003–2009, *J. Geophys. Res.*, *115*, D23115, doi:10.1029/2010JD014584.

1. Introduction

[2] The combined annual river discharge into the Arctic Ocean from Eurasian rivers has increased by 5–7% over the last 60 to 80 years [e.g., *Peterson et al.*, 2002; *Serreze and Etringer*, 2003; *Peterson et al.*, 2006; *Adam et al.*, 2007], and appears to be accelerating further over the last 20 years (A. Shiklomanov, River discharge, in Arctic Report Card 2009, http://www.arctic.noaa.gov/reportcard). Surface temperature observations and climate model simulations suggest that the Arctic regions respond more strongly to anthropogenic climate change compared to lower latitudes around the globe [*Serreze and Francis*, 2006; *Solomon et al.*, 2007]. In particular, it is expected that ongoing and future global warming increases the net poleward atmospheric moisture transport in conjunction with an acceleration of the global hydrological cycle [*Held and Soden*, 2006; *Solomon et al.*, 2007]. Various climate feedback mechanisms are linked to the storage and fluxes of water in the Arctic drainage basins [*Francis et al.*, 2009]. However, the role and response of the terrestrial water storage (TWS) balance to the large-scale climate changes has been elusive. Here, we analyze large-scale total TWS variations over the Eurasian Arctic from January 2003 to January 2010 as observed by the Gravity Recovery and Climate Experiment (GRACE) mission [*Tapley et al.*, 2004]. *Syed et al.* [2007] first used GRACE data over the Artic drainage region to determine basin discharge into the Arctic Ocean.

[3] River discharge is the dominant source of freshwater imported into the Arctic Ocean [*Serreze et al.*, 2006]. Recent extreme events like the 2007 sea ice minimum are interpreted as evidences of the dramatic changes, which, at least in the case of sea ice, appear to occur faster than projected by climate model simulations [*Stroeve et al.*, 2007], highlighting the sensitivity of the region to external forcing. Additional fresh water could significantly alter the Arctic Ocean freshwater budget, and could potentially have some ramifications on the deep water formation rates in the North Atlantic once it is exported from the Arctic through Fram Strait [*Peterson et al.*, 2002]. The Eurasian discharge area combined contributes about 74% to the total Arctic Ocean discharge [*McClelland et al.*, 2006]; the three largest Eurasian rivers Ob, Yenisei and Lena contribute on average about 57% to the total discharge in to the Arctic Ocean [*Serreze et al.*, 2006]. While the mean annual fresh water cycle of the Arctic river basins has been quantified based on direct observations and atmospheric reanalysis data [e.g.,

[1]Jet Propulsion Laboratory, California Institute of Technology, Pasadena, California, USA.
[2]Helmholtz Centre Potsdam, GFZ German Research Centre for Geosciences, Potsdam, Germany.

0148-0227/10/2010JD014584

Serreze et al., 2006], significant uncertainties still exist in terms of interannual variability and the contributions of long-term trends of TWS changes to discharge into the Arctic Ocean.

[4] Whether or not the observed increase of annual discharge from Eurasian rivers is consistent with changes of atmospheric moisture transport has been a topic of considerable attention in the literature [e.g., *Peterson et al.*, 2002; *Berezovskaya et al.*, 2004; *Peterson et al.*, 2006; *Smith et al.*, 2007; *Adam and Lettenmaier*, 2008]. On interannual to decadal time scales, it is often assumed that TWS changes are small and can be neglected in the hydrological budget [*Pavelsky and Smith*, 2006]. While this implies that the mean annual terrestrial discharge is in equilibrium with net precipitation (precipitation minus evapotranspiration) over the drainage regions, severe shortcomings in the observational record of precipitation, both in terms of sparse observations and undercatch problems, make it very challenging to extrapolate and attribute long-term changes to underlying large-scale forcing mechanisms in the Arctic region. To complicate matters, reservoir impoundments also affect the hydrological budget, in particular the phasing of the seasonal terrestrial water budget [e.g., *Shiklomanov and Lammers*, 2009].

[5] In the Arctic region, TWS is an important player in the phasing of the annual water budget. Seasonal discharge is strongly shaped by water storage in the snowpack. Flows are at a minimum in winter and typically peak in June. Another peculiarity of the Eurasian Arctic drainage basins is the existence of permafrost, especially over the eastern parts of the region. Permafrost is important for atmosphere-land interactions because of its large influence on the thermal and hydrological soil properties that also determine the runoff behavior. Due to the widespread temperature increases over pan-Arctic drainage basins, the region's expansive permafrost coverage is susceptible to change. Thawing permafrost can have partially offsetting effects on soil moisture and groundwater. On the one hand, the storage capacity of the soil may increase substantially through an increase of the active layer thickness (ALT) when permafrost soil thaws, which can also connect the surface layers with deeper water reservoirs. This permeability increase would tend to slow runoff. On the other hand, soil drainage may be improved and runoff from snow melt can potentially occur faster. These opposing responses may actually occur subsequently and represent the transient response of warming and thawing permafrost, but the time scales involved are uncertain. *Smith et al.* [2005] found that over continuous permafrost areas, the total open surface water area increased, while in discontinuous permafrost areas, the open surface water area declined. This would imply a diffuse lake drainage front where warming permafrost first experiences widespread degradation. However, it remains unclear how the total amount of terrestrial water and the water balance in a drainage basin is affected by permafrost changes. Rising minimum river flows in the region during the cold season are consistent with a broad-scale mobilization of groundwater and unsaturated zone inputs to river discharge through reduced ground freezing [*Adam et al.*, 2007; *Smith et al.*, 2007]. The maximum seasonal runoff during spring over the course from 1960 to 2001 has also been observed to occur earlier by several days [*Shiklomanov et al.*, 2007]. These effects, however, are limited to the seasonality of discharge. Interannual variations and positive discharge trends (based on observations since 1936) occur also in regions of little or no permafrost coverage, and are therefore not linked to permafrost change [*Pavelsky and Smith*, 2006; *McClelland et al.*, 2004].

[6] The conundrum of discharge increases that are unmatched by precipitation increases, in particular over the permafrost-covered eastern Eurasian basins, has led to speculations about alternative sources that can provide the missing discharge. It has been suggested that one of the principal controls could be permafrost thaw and melt of excess ground ice, especially in areas where discontinuous or sporadic permafrost may be more susceptible to change [*Serreze and Etringer*, 2003; *Serreze et al.*, 2006; *Adam and Lettenmaier*, 2008]. In this scenario, excess ground ice, which is abundant in volume compared to observed discharge increases [*McClelland et al.*, 2004], would melt and provide the missing discharge source. Since GRACE observes the total TWS, it allows us to assess the role of TWS variations on a basin-wide scale to investigate any missing discharge sources and possible permafrost contributions from a mass balance perspective.

[7] The objectives of our study are: (1) to quantify seasonal to interannual variations of TWS over the Eurasian pan-Arctic drainage basins based on GRACE observations; (2) to assess the individual contributions to the water budget over the pan-Arctic drainage region over the 2003–2009 time period by combining GRACE observations of TWS changes with atmospheric reanalysis data of net precipitation; (3) to infer the Eurasian basin discharge into the Arctic Ocean from GRACE and reanalysis data, and compare this to observed discharge from gauges; and (4) to assess if the observed TWS variations can be related to permafrost changes; in particular, if the discharge increase from the Lena basin can be related to the melting of the excess ground ice.

[8] In section 2, we present the data and methods used in the study. In section 3, we present observed and simulated TWS changes and the TWS budget in terms of contributing inflows and outflows over the GRACE time period. We discuss and summarize our results in section 4.

2. Methods and Data Sets

2.1. Terrestrial Water Budget

[9] Our analysis is based on the standard combined atmosphere-land water balance equation [e.g., *Serreze et al.*, 2006],

$$\frac{\delta S}{\delta t} = -\left(\frac{\delta W}{\delta t} + \nabla Q\right) - R, \tag{1}$$

where R is discharge, S TWS, W the vertically integrated atmospheric water vapor anomaly, and $\nabla(Q)$ the horizontal divergence of the vertically integrated atmospheric moisture transport. The atmospheric branch $-(\frac{\delta W}{\delta t} + \nabla Q)$ in equation (1) is referred to as the aerological budget and is, in principal, equal to precipitation minus evapotranspiration (P-ET). Here, we use column-integrated water vapor fields to compute $\frac{\delta W}{\delta t}$, and the column-integrated meridional and zonal water vapor fluxes for ∇Q from the Japanese

Re-Analysis data set JRA-25 [*Onogi et al.*, 2007] on the original T-106 grid. The TWS term is inferred from time-variable gravity as measured by GRACE (section 2.2). All derived quantities are interpolated onto a 1 × 1 latitude-longitude grid, and averages over hydrological drainage basin are based on the STN30 river network data set [*Vörösmarty et al.*, 2000]. As a reference, we use in situ observations of discharge R_{obs} from the ArcticRIMS project (http://rims.unh.edu/data.shtml; most of the discharge data for the analysis time period are provisional). Note that some fraction of the basin discharge may bypass the gauging stations and flow into the ocean unaccounted for by in situ gauges, adding uncertainty to these measurements [*Alsdorf and Lettenmaier*, 2003].

[10] GRACE provides monthly mean TWS anomalies. Therefore, the instantaneous water balance in equation (1) has to be adjusted to reflect this temporal sampling. Since the GRACE record is continuous (except for 06-2003, which we linearly interpolate from the previous and following months), we can use monthly mean values of P-ET and R, and the difference ΔS_{T2-T1} of monthly GRACE TWS anomalies is equal to [e.g., *Swenson and Wahr*, 2006a]

$$\Delta S_{T2-T1} = (F_1 + F_2)\frac{1}{2}, \tag{2}$$

where $F_{1/2}$ are placeholders for the monthly mean fluxes of P-ET and R. Due to errors and measurement uncertainties in the GRACE data, the approximation of ΔS_{T2-T1} by simple forward or backward differences introduces considerable high-frequency artifacts. To overcome this problem, we use centered differences for the rates of basin mean TWS anomalies. In order to match this central difference appropriately, the right-hand side of equation (1) must be computed as

$$\Delta S_i = \frac{1}{4}F_{i-1} + \frac{1}{2}F_i + \frac{1}{4}F_{i+1}, \tag{3}$$

where the indices $(i-1, i, i+1)$ refer to the previous, current, and following month, respectively. This is essentially a smoothing operation to reduce noise, but it comes at the price of reduced time resolution. Regardless of computing centered or simple differences, the pertinent point is that when using equation (1) with monthly mean GRACE data, the resulting fluxes always represent a mean flux over a minimum of at least two complete consecutive months. In contrast to *Syed et al.* [2007], we have found that when not accounting for this temporal sampling properly, the closure between flux terms in equation (1) can be substantially degraded, in particular over the current region of investigation where the TWS is strongly affected by the rapid spring snow melt.

2.2. GRACE Data Processing

[11] GRACE provides indirect estimates of mass anomalies near the Earth's surface by measuring the associated small variations of the geopotential field at an altitude of 458 km above the ground [*Tapley et al.*, 2004]. Here, we use GRACE Release 4.1 spherical harmonic coefficients from the Jet Propulsion Laboratory (JPL-RL4.1, available from http://podaac.jpl.nasa.gov/grace) up to degree and order 60. We adjust for correlated errors in the GRACE observations by postprocessing the data according to *Swenson and Wahr* [2006b], with a filter width of 5 degrees for spherical harmonic orders above 7 [*Duan et al.*, 2009]. Additionally, we replace geocenter estimates with those from *Swenson et al.* [2008], and substitute the C20 coefficient with measurements from Satellite Laser Ranging [*Cheng and Tapley*, 2004]. Postglacial rebound is corrected for based on the model of *Paulson et al.* [2007]. All GRACE TWS anomalies are relative to the time mean of January 2005 to December 2008. For spatial maps of TWS anomalies, the spherical harmonic coefficients are smoothed with a Gaussian averaging kernel of 250 km half width, and then expanded onto a regular latitude-longitude grid at 1 degree resolution [*Wahr et al.*, 1998]. We compute basin averages using an unsmoothed exact averaging kernel, truncated at spherical harmonic degree 60. While this choice of averaging kernel can lead to spurious signals for small basins [e.g., *Swenson and Wahr*, 2003; *Klees et al.*, 2007; *Chen et al.*, 2007], we found that additional smoothing of the kernel has little effect on the computed basin averages. Additionally, the applied destriping and spectral truncation attenuates true geophysical signals. We estimated these biases by applying the same destriping, truncation and spatial averaging to synthetic TWS data from the GLDAS-NOAH model [*Rodell et al.*, 2004], and calculated scaling factors to match the original amplitudes in a least squares sense. The scaling factors are small and range from 1.0 to 1.09 for the choice of processing parameters used here (see Figure 1 for basin values).

[12] Errors in GRACE water storage estimates are due to satellite errors, processing errors, and errors in the background and dealiasing fields used. Since the calibrated errors provided from GRACE are likely not representative of the true error, we fit a trend, annual and semiannual term to GRACE coefficients, and interpret the residuals as an empirical conservative error estimate [*Wahr et al.*, 2006]. This approach works well if interannual variations are small, but since longer period variations emerge in the GRACE record, the residuals would tend to overestimate errors. Therefore, we use the same approach as *Wahr et al.* [2006] but only fit in a moving window of 2 years. From these residuals, we compute the root-mean-square (RMS) and use these as representative errors. The RMS values for the mean monthly TWS anomalies across individual drainage basins range from 0.7 to 1.1 cm, and are lower for larger averaging regions.

[13] Errors of the discharge observations are not well constrained, but are likely at least on the order of 10%, with higher uncertainty during winter months due to the presence of ice [*Serreze et al.*, 2002]. Similarly, errors in the reanalysis moisture fluxes are also poorly constrained in lack of independent observations. Relative differences of aerological fluxes between different reanalysis products are on the order of up to 10% (e.g., between JRA-25 and ERA-Interim), but due to the common observational data assimilated in different reanalysis products, systematic biases cannot be discerned. Here, we use a relative error estimate of 10% for P-ET, similar to previous studies [e.g., *Serreze et al.*, 2006]. All error terms are then combined by propagation through equation (1).

3. Results

3.1. Stocks: TWS From GRACE 2003–2009

[14] The area-average TWS over the entire Eurasian pan-Arctic drainage region has a seasonal peak-to-peak ampli-

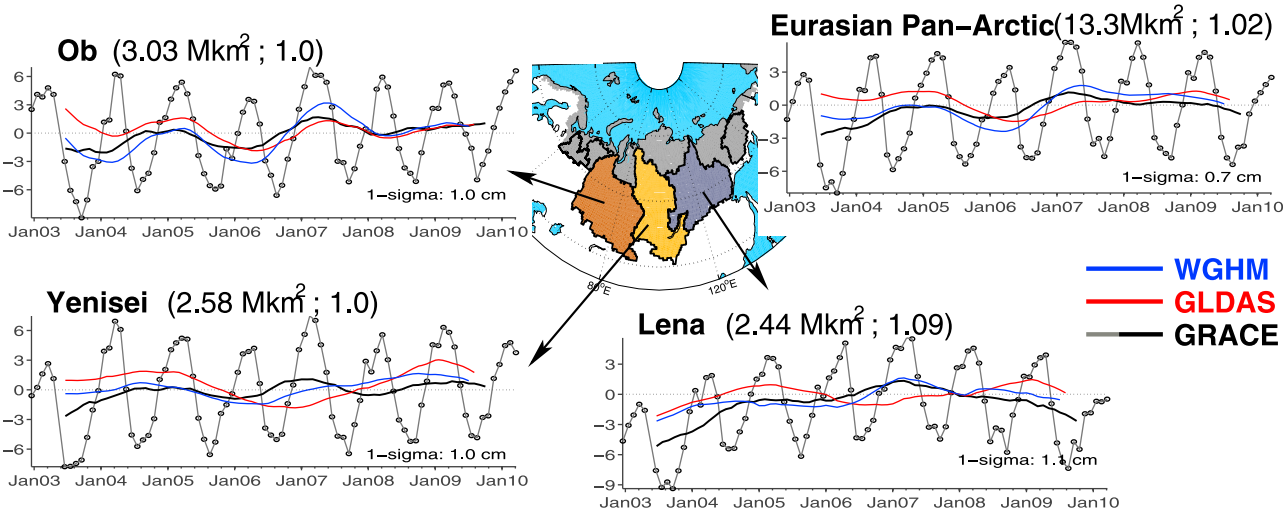

Figure 1. Basin-mean terrestrial water storage (TWS) anomalies from GRACE for the total Eurasian pan-Arctic drainage area (encompassing the big three river basins and the grey shaded area), the Ob, Yenisei, and Lena River basins. Anomalies are relative to the 2005–2008 time mean, in centimeters of water-equivalent height. Black and grey lines are monthly mean TWS and 12 month running mean TWS from GRACE, respectively. Blue and red lines are 12 month running mean TWS from the hydrology models WGHM and GLDAS-NOAH, respectively. The basin size and the scaling factors as determined from GLDAS-NOAH are given in brackets (see section 2 for details). Uncertainty estimates (1-σ level) for the TWS anomalies from GRACE are given in each panel.

tude of 10.6 cm, with similar values over the largest basins (Ob: 12.3 cm; Yenisei: 12.4 cm; Lena: 10.1 cm). Maximum TWS typically occurs in May, declines rapidly in boreal spring when snow melt sets in, and thereafter gradually reduces to its seasonal minimum between August and October (Figure 1). Over the GRACE time period, the TWS over all basins exhibits significant interannual variability. Such variability can arise from changes in net precipitation or discharge. An increase in TWS would be consistent with either an increase in P-ET, or a decrease in R; conversely, a decrease in TWS would require reduced P-ET or increased R (equation (1)). Additionally, changes of the TWS capacity through changes of soil properties can affect runoff, and also land-atmosphere fluxes through ET.

[15] For the Ob and Yenisei basin, as well as the Eurasian pan-Arctic watershed as a whole, there is a tendency for overall TWS increase from 2003 to 2009 (Figure 1). However, fitting a linear trend to the basin mean TWS is not warranted given the apparent interannual variations and the short record of observations. A seasonal Mann-Kendall trend test, adjusted for autocorrelation [*Hirsch and Slack*, 1984], reveals that linear trends fitted to the mean TWS in the Lena and Ob basins, as well as the total Eurasian watershed, are statistically not significant at the 95% level. Only for the Yenisei Basin is the linear trend of 0.32 cm/yr significant at 95% but rather small in amplitude. The data record, while short, suggests the presence of low-frequency variations of 2–2.5 years, which has also been reported for other large river basins [*Schmidt et al.*, 2008]. Similar interannual TWS variations are also simulated with hydrological models, and therefore are likely caused by variations in the forcing of TWS anomalies (P or ET). Whether robust physical connections between the interannual variations and large-scale climate variations such as the Arctic Oscillation exist is still unclear [*Serreze and Barry*, 2005; *Krokhin and Luxemburg*, 2007], and considerably longer time series are needed to assess statistical significances. Compared to the Ob and Yenisei basins, the TWS over the Lena basin increased considerably more from 2003 to early 2007, but since early 2007 this signal has reversed sign. This quasi-trend behavior is at least qualitatively consistent with variations in P-ET over the Lena basin, which had a similar declining signal since 2007 (see detailed analysis of TWS controls in section 3.2). The spatial distribution of TWS trends over the entire time period from 2003 to 2009 reveals large-scale positive TWS trends (Figure 2a), but no continuous colocation between those trends and regions of permafrost (Figure 2c). For the Ob, Yenisei and the regions west of the Ob, the maximum increase is concentrated to the south of the permafrost areas in a band that spans the northern and middle parts of the basins. In the central Lena basin, the trend is colocated with areas of mostly discontinuous permafrost. The seasonal Mann-Kendall test reveals that a considerable fraction of the local trends above about 1 cm water-equivalent height are significant at the 95% level (Figure 2b).

[16] In order to gain more insight into the spatiotemporal pattern of the nonseasonal TWS variations, we compute empirical orthogonal functions (EOFs) of the data [e.g., *Hannachi et al.*, 2007] after subtracting a composite seasonal cycle from each grid point anomaly. The different EOF modes need not necessarily represent independent physical modes [e.g., *Dommenget and Latif*, 2002], and due to the short record length, the EOF/PC may change with a longer record. Sensitivity test on GRACE TWS show that the EOF/PC patterns do not change significantly if at least 60 months are used (not shown). The primary use of the EOF decomposition here is to reveal the centers of action of

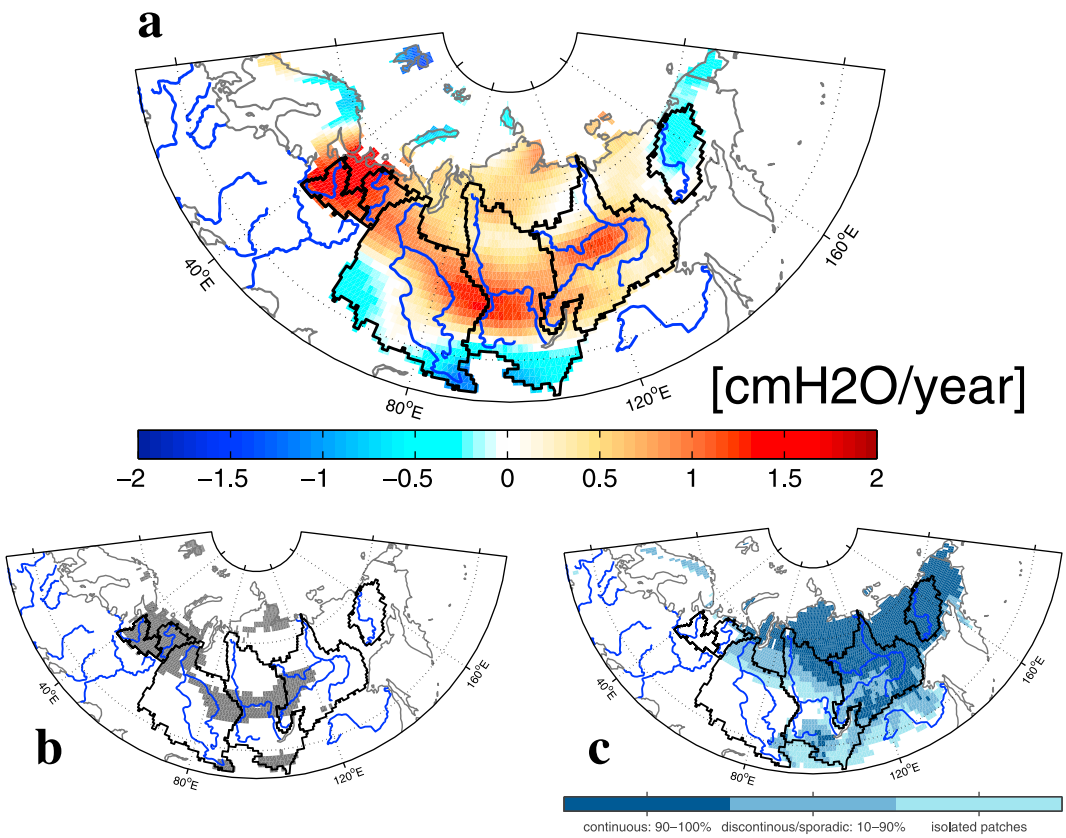

Figure 2. (a) Trend component of terrestrial water storage over Eurasian drainage region (in cm of water/yr) calculated by simultaneously fitting constant, trend, annual, and semiannual as well as GRACE-specific aliasing periods of 161 and 1362.7 days [*Ray and Luthcke*, 2006] to the GRACE data from January 2003 to January 2010. (b) Grey-shaded areas show regions where the linear trend is significant at the 95% level based on a seasonal Mann-Kendall test, accounting for serial correlation [*Hirsch and Slack*, 1984]. (c) Permafrost distribution over the region [*Brown et al.*, 1998].

nonseasonal variations, to assess if these signals are collocated to regions of permafrost or related to anomaly patterns in the controls of TWS anomalies, and to facilitate a comparison of TWS simulated with state-of-the-art hydrology models.

[17] The EOF/PC decomposition of the entire drainage region (Figure 3) yields a first mode that extends across all basins, but lumps together different temporal variability of the individual basins. Therefore, we compute the EOF for each basin individually. The first EOF/PC modes of the three large basins show distinctively different behavior, in particular between the Ob and Lena basin, while the Yenisei comprises features of both extremes (Figure 3). The explained variances for the first mode range from 43 to 71%. About 4–10% of the Ob basin is underlain by permafrost, which gradually increases to 36–55% of the Yenisei basin, and to nearly complete coverage of 78–93% for the Lena basin. Since permafrost is largely absent in the Ob basin, the observed TWS anomalies cannot be related to changes in permafrost. Similarly, the changes in the Yenisei basin are centered over the nonpermafrost regions, and thus also not related to permafrost-specific TWS dynamics. The prominent variations with a period of 2 to 2.5 years in the principal component time series of Ob and Yenisei suggest a common atmospheric driving process or TWS response leading to the observed nonseasonal TWS anomalies, while the first EOF/PC mode of the Lena basin shows a relatively monotonous TWS increase until early 2007, and a weaker decline after 2007 (Figure 3). The strongest TWS increase occurred in 2004. That year is actually marked by comparatively low P-ET, with corresponding low discharge values based on gauge observations. The scenario of increasing TWS during decreasing P-ET invites speculations about TWS capacity changes in the Lena basin. Could permafrost thaw have expanded TWS capacities to account for the observed increase? In lack of direct large-scale observations, the answer remains speculative. Degradation of permafrost in the East Siberian regions has been documented based on in situ observations from 1930 through 1996 [*Romanovsky et al.*, 2007], and with unabated warming over the last decade, it is likely that the subsurface ground has warmed even further. Additionally, winter snow thickness also plays an important role for subsurface temperatures. Thicker layers of snow in winter months effectively insulate the ground to prevent heat loss to the atmosphere, which also inhibits recovery of previously degraded permafrost. However, as surface and subsurface temperatures are only weakly correlated on time scales of less than 10 years [*Romanovsky et al.*, 2007], TWS variations from GRACE are likely not strongly linked to concurrent surface tem-

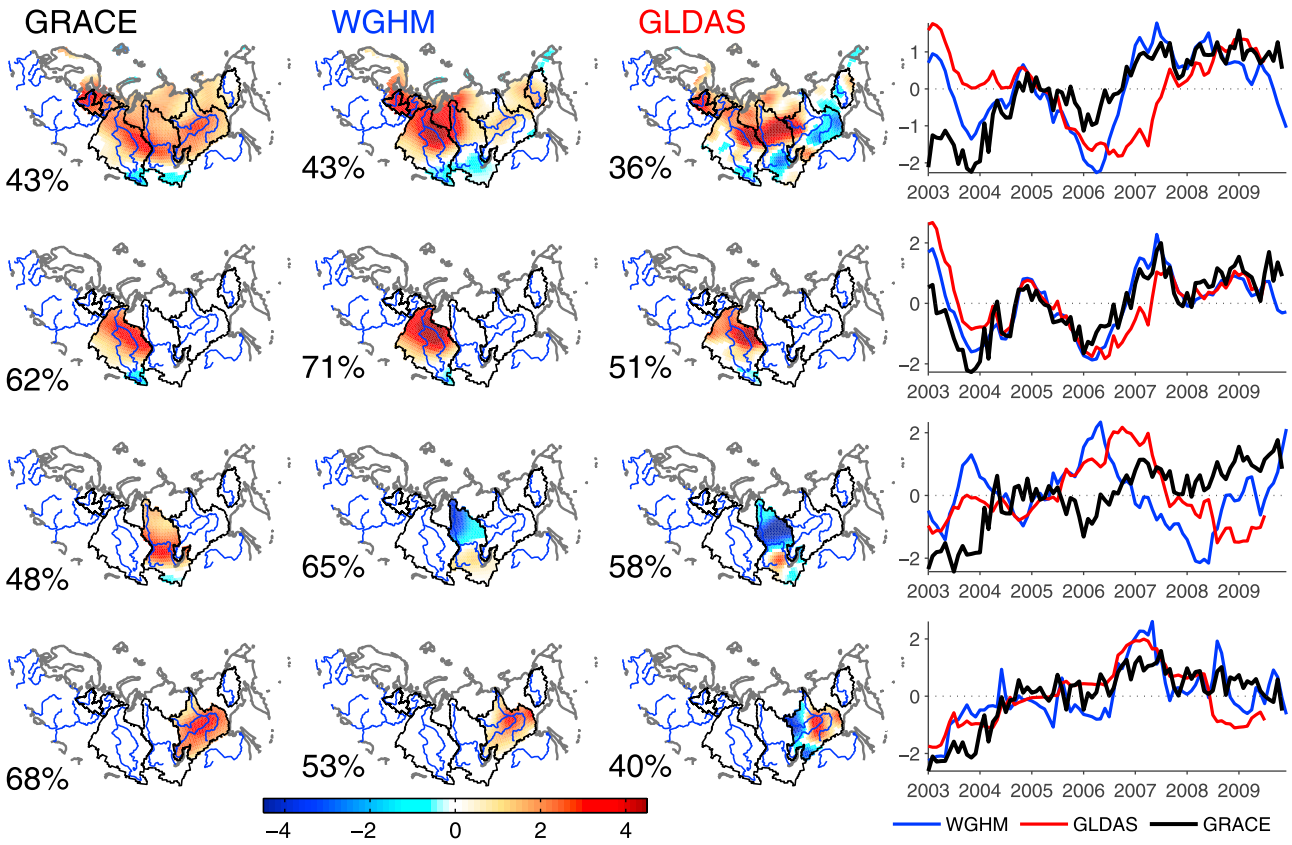

Figure 3. Mode 1 of the EOF/PC decomposition of the terrestrial water storage (TWS) anomalies (composite seasonal cycle subtracted) from GRACE, WGHM, and GLDAS-NOAH for total (top to bottom) Eurasian pan-Arctic, Ob, Yenisei, and Lena. The explained variance is given in each map as percentage of total variance. The PC time series at right are normalized by their standard variations, and the EOF spatial maps are scaled by the same factor. The units for the EOF spatial maps are in centimeters of water-equivalent height.

perature variations. This notion is supported by the lack of significant correlation between the nonseasonal surface temperature anomalies from JRA-25 and TWS anomalies from GRACE (not shown).

[18] For the second EOF modes, the Yenisei and Lena exhibit a similar spatiotemporal behavior. The explained variances for this mode range from 12% to 33% (Figure 4). The second PC is dominated by events starting in 2007 lasting through 2009, as well as some energy at the beginning of the record in 2003. Spatially, the second EOF/PC is concentrated along the southern and northern edges of the basins with opposing signs. This spatial structure is at least partly due to the orthogonality constraint in the EOF/PC decomposition. However, the rotated EOF patterns did not change significantly, so they appear to be robust. The declining TWS in the southern parts of the basins and increasing TWS in the northern parts of the basins during 2007 is consistent with the observed anomalous precipitation pattern during 2007 [*Shiklomanov and Lammers*, 2009; *Rawlins et al.*, 2009a], which is linked to an anomalous circulation pattern of low pressure over western and central Eurasia, in turn possibly related to a positive NAO phase [*Rawlins et al.*, 2009a]. The reversal of the 2007 TWS signal starting in early 2008 suggests a common atmospheric change in P-ET in those areas.

[19] In the absence of any independent observations to which the GRACE observations can be compared against, we use data from two hydrology models to assess the TWS signals to gain some additional insight into the GRACE observations. The models used are the conceptual Watergap Global Hydrology Model (WGHM) [*Döll et al.*, 2003] and the Land Surface Model NOAH running within the Global Land-Data Assimilation System (GLDAS-NOAH) [*Rodell et al.*, 2004]. WGHM has water storage components for snow, soil moisture, groundwater and surface water in the river network, lakes and wetlands, whereas GLDAS-NOAH does not explicitly simulate groundwater and surface water. WGHM uses a heuristic approach to reduce groundwater recharge in permafrost areas, depending on the permafrost spatial extent and type (continuous, discontinuous, sporadic permafrost) in each 0.5 degree model cell [*Döll and Fiedler*, 2008]. GLDAS-NOAH includes a frozen soil scheme [*Koren et al.*, 1999] for soil layers down to a depth of 2 m mainly to represent the latent heat balance of freezing and thawing top soil. Neither model, however, explicitly represents permafrost processes or temporal permafrost dynamics, such as permafrost extent, type, or active layer thickness.

[20] Simulated water storage variations reasonably match the GRACE TWS observations (compare interannual variations in Figure 1). TWS from WGHM tends to match the

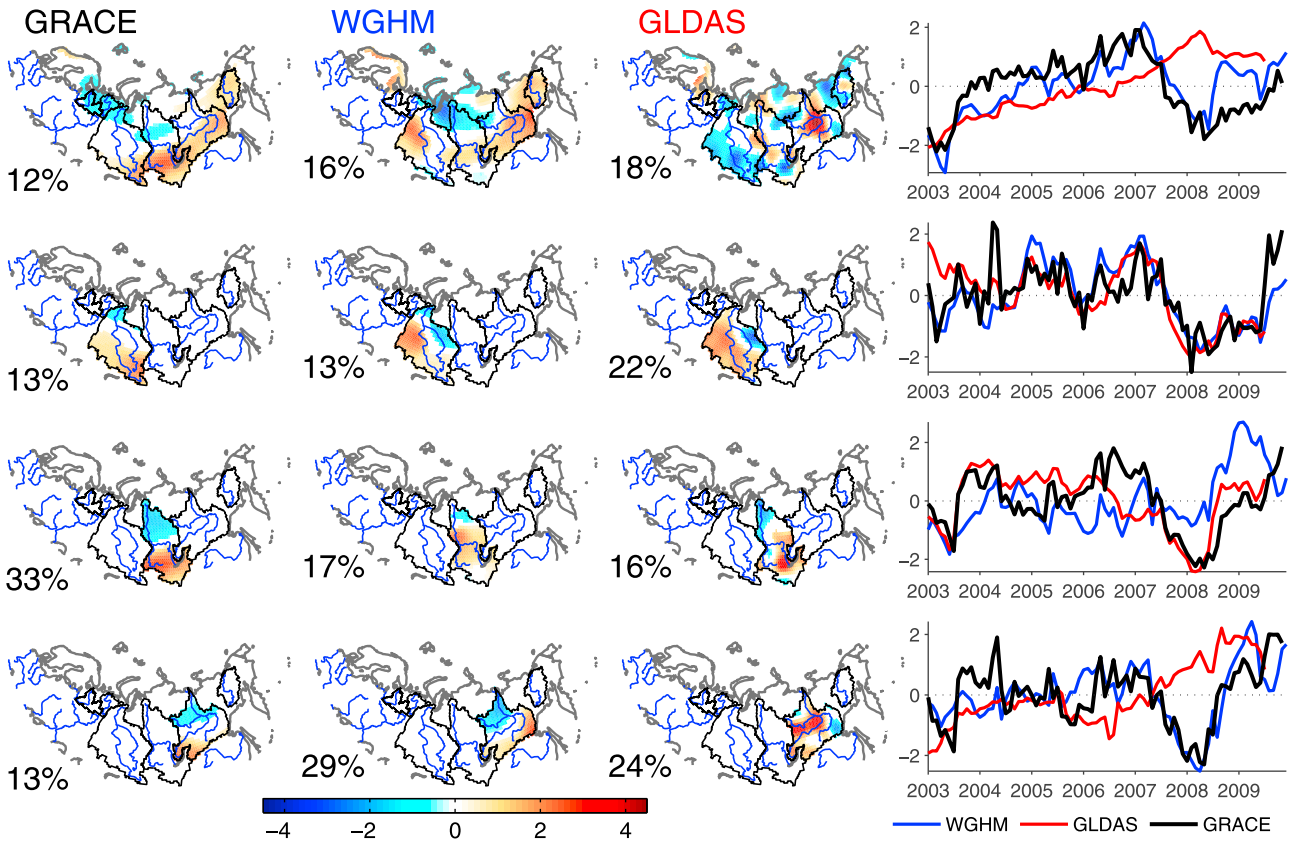

Figure 4. Mode 2 of the EOF/PC decomposition of the terrestrial water storage (TWS) anomalies from GRACE, WGHM, and GLDAS-NOAH for total (top to bottom) Eurasian pan-Arctic, Ob, Yenisei, and Lena. See Figure 3 for details.

GRACE data better than GLDAS-NOAH, both in terms of a lower root-mean-square difference as well as a higher correlation (Figure 5). For the Ob basin, the nonseasonal spatiotemporal TWS patterns of GRACE and the models agree very well, both for EOF/PC 1 and 2 (Figures 3 and 4). The EOF correspondence is less favorable for the Yenisei basin, with considerable differences both between GRACE and the models and also between the two models. However, the dominant event in the second EOF/PC of the Yenisei from 2007 to 2009 mentioned above is similarly captured by GLDAS-NOAH while it is represented in the first EOF/PC by WGHM (Figures 3 and 4). In the Lena basin, GRACE and WGHM show a similar trend-like pattern in the first EOF/PC, while this feature is split between mode 1 and 2 for GLDAS-NOAH (Figures 3 and 4).

[21] Differences between the models in simulating interannual TWS variations can be due to a variety of factors including model structure and driving forces, with precipitation input being among the most important [e.g., *Slater et al.*, 2007]. As WGHM is driven by GPCC precipitation [*Rudolf and Schneider*, 2004] and GLDAS-NOAH by Climate Prediction Center Merged Analysis of Precipitation (CMAP) fields, intermodel differences can be caused by differences of these data sets, and deficiencies in the precipitation data sets may propagate into considerable mismatch of simulated TWS relative to GRACE TWS. The effect of differences in input data may exceed the effect of different storage components represented by the models, i.e., model structure. For EOF/PC patterns of mode 1, WGHM(TWS) and WGHM(snow+soil moisture) are more similar to each other and GRACE than is GLDAS(snow+soil moisture) to WGHM(snow+soil moisture) or GRACE (not shown). Thus, one cannot simply attribute the better match of WGHM and GRACE to the inclusion of groundwater and surface water storage in WGHM. Although these are two important storage components with different seasonal dynamics compared to snow and soil moisture storage in the study area [*Güntner et al.*, 2007], their effect is less relevant for the interannual storage variations analyzed here, where differences in climate forcing data may obviously be more important for explaining the differences between GLDAS-NOAH and WGHM. In spite of the model differences, the EOF/PC decomposition of simulated nonseasonal TWS shows that the models are able to capture important features of the interannual GRACE TWS signal. The models are successful in this by using climate forcing as the only time-variable constraint to the model simulations, ignoring any seasonal or longer-term permafrost dynamics. These results give additional evidence that the observed water storage variations in the Eurasian pan-Arctic from GRACE are predominantly driven by variations of the P-ET budget.

3.2. Flows: Hydrological Budget in 2003–2009

[22] In this section, we assess the seasonal and nonseasonal variability of the budget terms in equation (1), and how well the different observational data sets close the

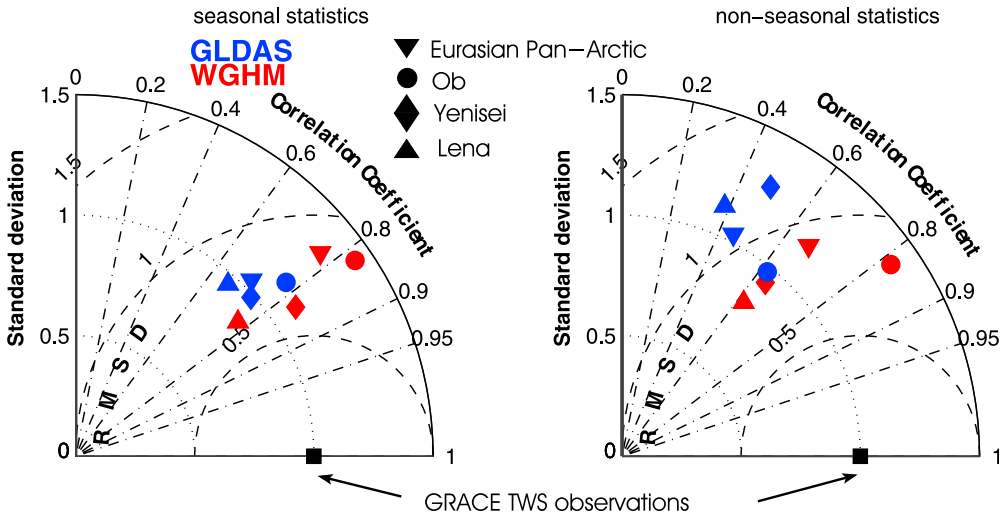

Figure 5. Taylor diagram [*Taylor*, 2001] summarizing the normalized statistics of the comparison of simulated TWS anomalies from GLDAS-NOAH and WGHM relative to the observed TWS anomalies from GRACE for the Eurasian pan-Arctic drainage region and the major drainage basins (time period January 2003 to December 2009). (left) Comparison of the full simulated time series; (right) comparison of nonseasonal variations (12 month moving averages). In both cases, WGHM has higher correlations with GRACE and tends to have a lower root-mean-square difference than GLDAS-NOAH (indicated by the distance from the observations). GLDAS-NOAH tends to match GRACE observations better in terms of the standard deviations. Note that the statistics here are normalized by the standard deviations of the GRACE observations and take into account the agreement of the spatial pattern as well as temporal behavior; the statistics of the basin-mean values only are very similar to the ones shown.

terrestrial Eurasian pan-Arctic water budget from 2003 to 2009. The seasonal variations of P-ET, P, R and ET have previously been quantified in several studies (see, e.g., *Serreze and Barry* [2005] for a summary), but the annual components of TWS change rates, dS/dt, have not due to the lack of direct, large-scale observations. Over longer periods, it is often assumed that TWS changes average out over nonglaciated regions (otherwise, there would be a net mass gain or loss in TWS). With observations from GRACE, we can now address the validity of this assumption, albeit the time series is still relatively short for hydrological applications where random fluctuations of P-ET or R can introduce long-term memory in TWS (because TWS is the integrated response to these fluxes). Nonetheless, the seasonal variations in TWS change rates on a basin scale from GRACE allow an independent assessment of the quality of the P-ET estimates and the measured basin discharge from gauges. Additionally, equation (1) represents an alternative to infer discharge over large drainage basins such as the Eurasian pan-Arctic, about one fourth of which is not or only poorly monitored with discharge gauges. Previously, the annual Eurasian pan-Arctic drainage basin discharge has been estimated at about 2970 km^3/yr (centered on the GRACE period) by scaling the monitored areas to account for the unmonitored regions [*McClelland et al.*, 2006]. Rearranging equation (1), the inferred discharge from JAR-25/GRACE yields a similar mean annual value of 2920 km^3/yr. This value is, of course, almost entirely determined by atmospheric moisture fluxes as annual TWS change rates are nearly 2 orders of magnitude smaller than the total P-ET.

[23] For seasonal variations, the relative amplitudes and phasing of P-ET and dS/dt over the basins reflect the milder and wetter climatic conditions in the western parts (Ob) compared to the colder and drier eastern regions (Lena). In the more eastern parts of the region, a larger fraction of the precipitation falls as snow that accumulates during the winter months and rapidly melts in spring, and seasonal P-ET and TWS changes are offset compared to the western regions (Figures 6b–6d). The seasonal cycle of TWS changes rates is similar over all basins, reaching maximum values in November/December, and minimum values in June (maximum TWS loss rate) when the snow melts. For the Ob basin, seasonal TWS rates and P-ET closely follow each other in phase and amplitude (Figure 6b). This is expected because 74% of the annual precipitation goes into evapotranspiration and consequently only the remaining fraction is available for discharge into the Arctic Ocean [*Serreze and Barry*, 2005]. During June and July, net P-ET for the Ob basin becomes negative and terrestrial water becomes a source for atmospheric water. Since a considerable fraction of the TWS in the Ob is in the form of open surface water in wetlands, ET is not limited by available soil moisture and occurs close to its potential rate [*Serreze and Barry*, 2005]. Over the Yenisei and Lena basins, on the other hand, only about 55% and 45%, respectively, of the annual precipitation is lost through evapotranspiration, and P-ET generally does not attain negative values during summer months (Figures 6c and 6d). Note that higher R/P ratios are found over permafrost regions because the permeability of the soil is limited [*Serreze and Barry*, 2005]. Additionally, colder mean temperatures over the permafrost regions result in

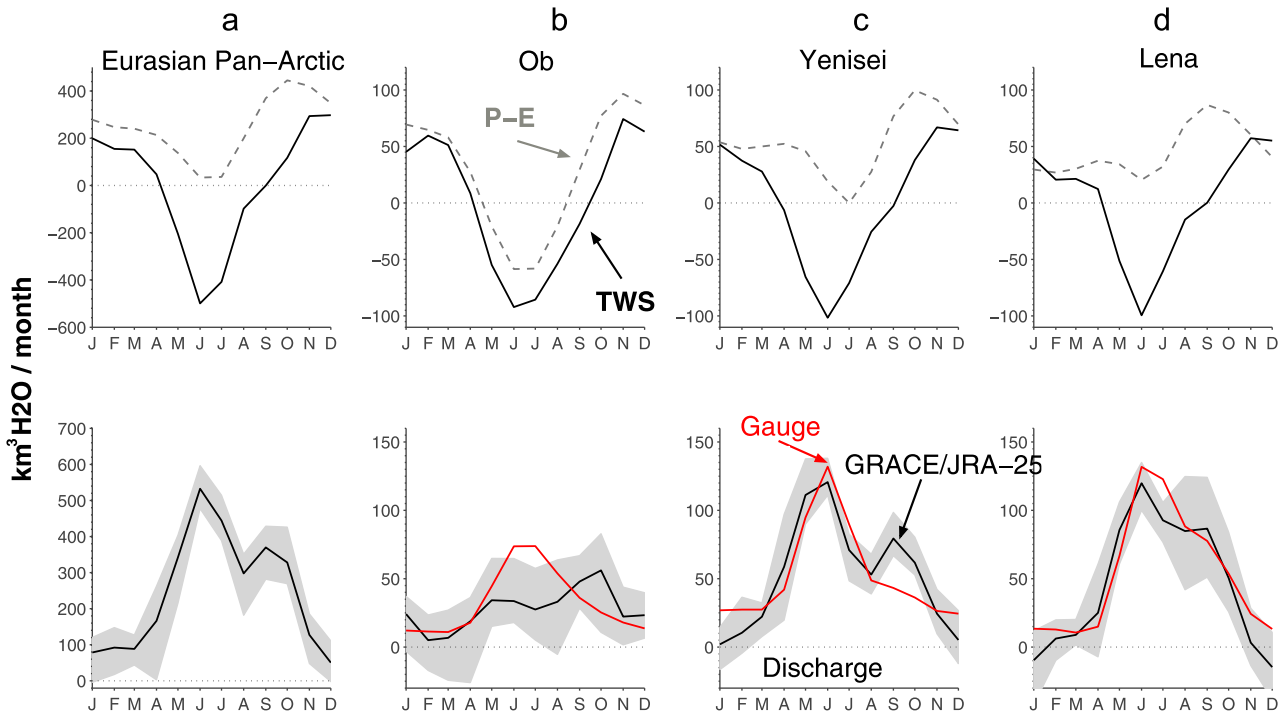

Figure 6. Climatology of monthly mean fluxes (shown in Figure 7). (top) TWS change rates from GRACE (solid line) and net precipitation P-ET from JRA-25 (dashed line). (bottom) Inferred discharge (with shaded uncertainty estimate, computed by solving equation (1) for R) and gauged discharge (red line, relative uncertainty 10%). Note that the monthly gauge observations have been smoothed to account for the temporal sampling from GRACE; see section 2 for details. The mean annual net precipitation P-ET for Eurasia from JRA-25 is 3150 km^3, while the mean annual inferred discharge is about 2920 km^3.

lower ET. The lower ratios of ET/P for the Yenisei and Lena, and the fact that P-ET and dS/dt are not in phase due to significant snow storage in winter result in a larger fraction of the precipitation going into runoff and discharge. Therefore, the inferred discharge estimate through the difference of P-ET and dS/dt has a higher signal-to-noise ratio for these two basins, whereas for the Ob, the inferred discharge is a comparatively small difference between two bigger components that are in phase. This causes the inferred discharge over the Ob basin to be in poor agreement with gauged discharge values (Figure 6). An additional error source for the Ob basin may come from the JPL-GRACE data set we use here to estimate TWS variations. Relative differences between the JPL-RL4.1 data set and other GRACE solutions (e.g., from the Center for Space Research, CSR) are bigger for the Ob basin than for the Yenisei and Lena on the seasonal time scale. The reasons for this are unclear and are under investigation. The inferred discharge estimates for the Yenisei and Lena basins (Figure 6) agree well with the gauge observations. The timing of the spring discharge coincides in both curves, but the inferred estimates are slightly below the gauge values. Bias-like differences exist in the late summer and winter months (discussed below).

[24] As described in section 2, we derive P-ET estimates from the aerological budget of JRA-25 reanalysis data. In Figure 7, the basin-averaged precipitation time series of the GPCP data set [*Adler et al.*, 2003] are also shown. From the difference to P-ET, one could infer ET (as, e.g., done by *Serreze and Etringer* [2003]), which is generally the least known budget parameter over land. Instead of inferring ET, we focus on the budget closure with dS/dt from GRACE and P-ET from JRA-25, and observed discharge from gauges. GRACE measurements are independent from R and P-ET observations, and therefore yield important large-scale information over the sparsely observed high northern latitudes. During the cold winter months, ET over most parts of northern Eurasia is very small, and discharge into the Arctic Ocean is also at its minimum [*Serreze and Etringer*, 2003]. In this respect it is reassuring that basin-averaged P-ET from JRA-25 is never larger than P from GPCP, and very close to GPCP during the winter months (Figure 7, dashed lines).

[25] When averaging over entire river basins, TWS rates dS/dt should always be equal to or smaller than P-ET in the absence of any other TWS sources (otherwise R in equation (1) becomes negative, which is obviously not possible as rivers do not run backward). However, during some months, we obtain TWS change rates dS/dt from GRACE that are larger than precipitation from GPCP or P-ET from JRA-25. For those months, the inferred basin discharge (solving equation (1) for R) becomes negative, which is unphysical. Over the Lena and Yenisei basins, this situation occurs consistently during the cold winter months. Although the propagated errors for the inferred discharge typically include the zero value, the consistently below-zero inferred dis-

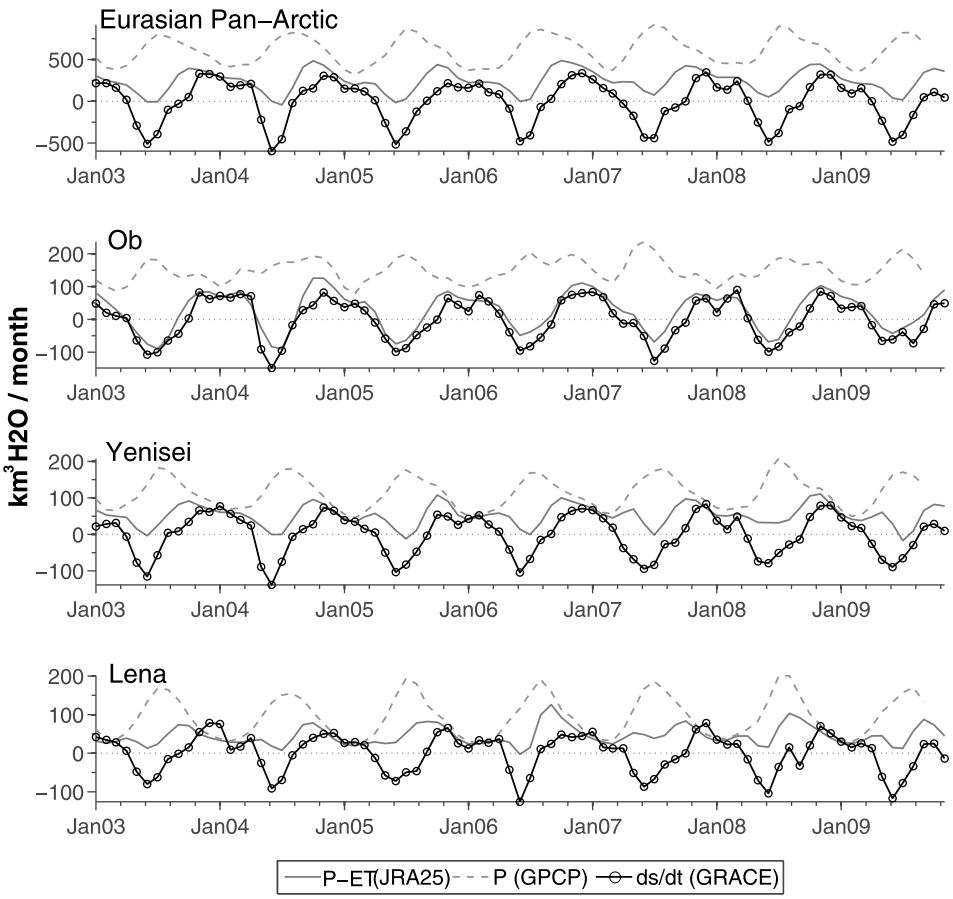

Figure 7. Monthly mean TWS change rates (black with circles), net precipitation P-ET from JRA-25 (solid grey line), and precipitation *P* from GPCP (dashed grey line) for (top to bottom) pan-Arctic Eurasia, Ob, Yenisei, and Lena river basins. Monthly values for P-ET and *P* have been matched to GRACE estimates of *dS*/*dt* according to equation (3).

charge values suggest the presence of a systematic bias (Figures 8c and 8d). Two scenarios could explain the discrepancies: either GRACE overestimates the mass gain during some winter months, or the basin-integrated precipitation is underestimated in the observations (which then also propagates into P-ET from JRA-25). It is difficult to explain why GRACE would consistently overestimate the mass gain during some winter months for the Yenisei and Lena. The spatial patterns of the TWS anomalies from GRACE could have some influence on the basin-integrated TWS amplitudes through spatial signal leakage [*Swenson and Wahr*, 2002]. However, we have evaluated several different averaging kernels, but they do not significantly affect the estimated TWS change rates. The leakage issue for GRACE data is not critical for the basins examined here as TWS anomalies tend to be of similar amplitude and in phase across basin boundaries [*Klees et al.*, 2007]. Therefore, underestimation of basin-integrated net precipitation might cause the negative inferred winter discharge, but this is difficult to assess in lack of independent observations. Alternative reanalysis data (NCEP/NCAR aerological fluxes, as well as ERA-Interim forecast P-ET) also result in negative discharge estimates during some cold winter months. However, the reanalysis products assimilate similar atmospheric observations and therefore likely contain similar biases. A bias in the inferred discharge of opposite sign tends to occur during the late summer months of September and October, in particular for the Yenisei basin, but also over the Lena (Figures 8c and 8d). Here, the inferred late-summer GRACE/JRA-25 discharge is consistently larger than the gauge measurements. Again, this signal is also present when we use NCEP/NCAR or ERA-Interim P-ET estimates. During some years, a secondary discharge peak is also seen in the gauge measurements, but it is usually smaller than the secondary peak in the inferred discharge, and mostly not present at all during the GRACE period. Interestingly, hydrological models also tend to have a second discharge peak during September and October for these river basins [*Slater et al.*, 2007; *Werth and Güntner*, 2010]. During those months, P-ET reaches its annual maximum, and precipitation is typically in the form of rain. Additionally, it is possible that a considerable amount of runoff bypasses the streams and is not accounted for by the installed gauges [*Syed et al.*, 2007]. Alternatively, P-ET in the reanalysis data sets could be overestimated either by too much precipitation or too little evapotranspiration. Either hypothesis is speculative at this point, but should be further investigated. Besides naturally occurring variations, artificial reservoir impoundments can also affect the hydrological budget. While impoundments over the Eurasian Arctic

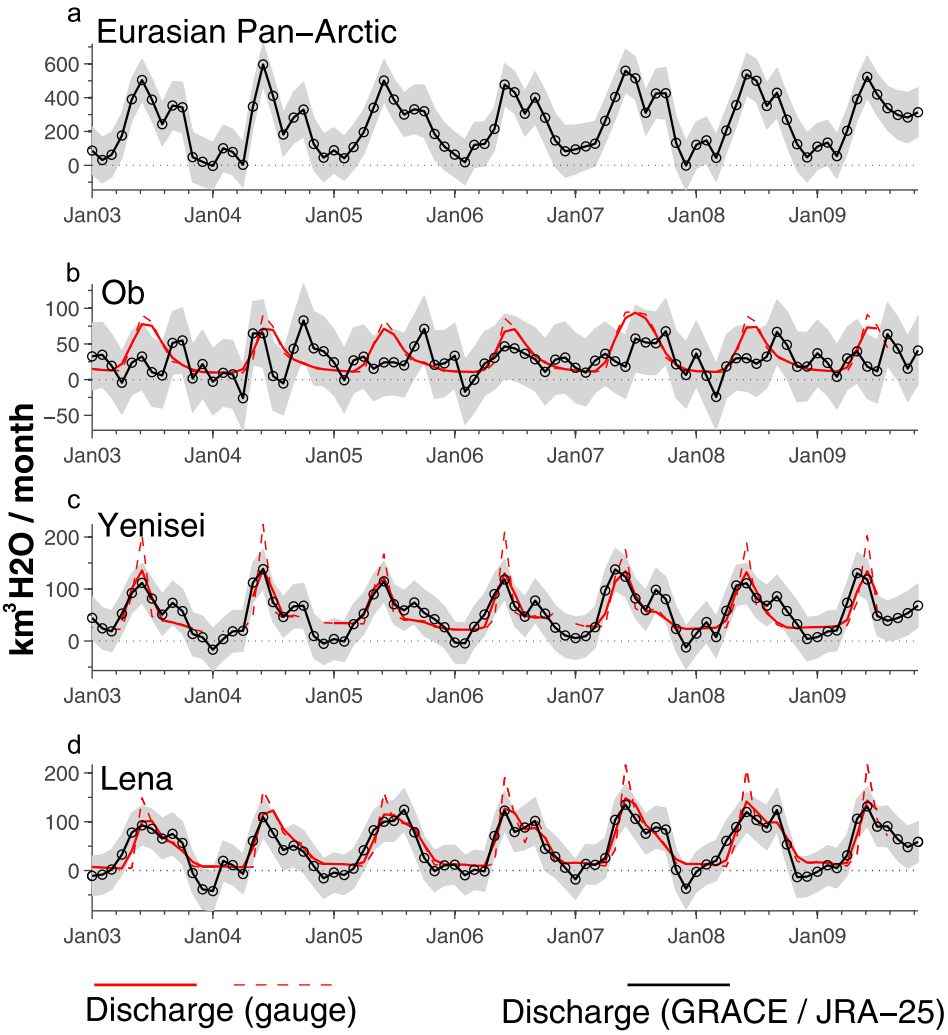

Figure 8. Monthly mean basin discharge inferred from GRACE/JRA-25 and directly observed (where available). Observed discharge is from the ArcticRIMS project; the red dashed lines are the original monthly discharge observations, and the red solid lines are the monthly discharge observations matched to GRACE estimates of *dS*/*dt* according to equation (3).

basins have significantly influenced the phasing of the seasonal terrestrial water budget [e.g., *Shiklomanov and Lammers*, 2009], the inferred discharge biases (from GRACE and JRA25) cannot be attributed to dams because water storage changes in reservoirs affect the GRACE signal and are thus implicitly accounted for in the budgeting applied here.

[26] Finally, we assess the budget closure of non-seasonal and interannual variations to shed some light on the conundrum of stream flow trends exceeding observed precipitation trends [*Adam and Lettenmaier*, 2008]. We computed annually accumulated fluxes of the observed quantities *dS*/*dt*, P-ET, and *R* by summing the monthly values in a 12 month moving window (Figure 9). Again, any trends should be treated with caution given the short GRACE record. For the milder western regions, most variability in P-ET is expected to be reflected in TWS changes due to the low runoff ratio. This is indeed the case for the Ob basin, where the interannual TWS change rates agree very well with net precipitation anomalies (Figure 9b). With the exception of 2007, annual discharge from gauges in the Ob does not exhibit any trends or significant interannual variability from 2003 to 2009. Although nonseasonal *dS*/*dt* and P-ET over the Ob basin agree well, the inferred discharge exhibits considerably more variability compared to the gauged discharge estimate, which may at least partly be due to TWS errors mentioned above. Moving farther east into the Yenisei basin, the correspondence between interannual variations of *dS*/*dt* and P-ET begins to vanish as discharge variations become more important with the increasing *R*/*P* ratio [*Serreze and Barry*, 2005], but due to missing provisional gauge observations for some months we cannot reliably assess the closure of the interannual budget over the Yenisei basin. The larger discrepancy between annual P-ET and *dS*/*dt* from 2007 to 2008 is consistent with the record discharge in 2007, such that a positive P-ET anomaly mainly fed runoff and discharge, and had less effect on TWS. The annually accumulated fluxes over the cold Lena

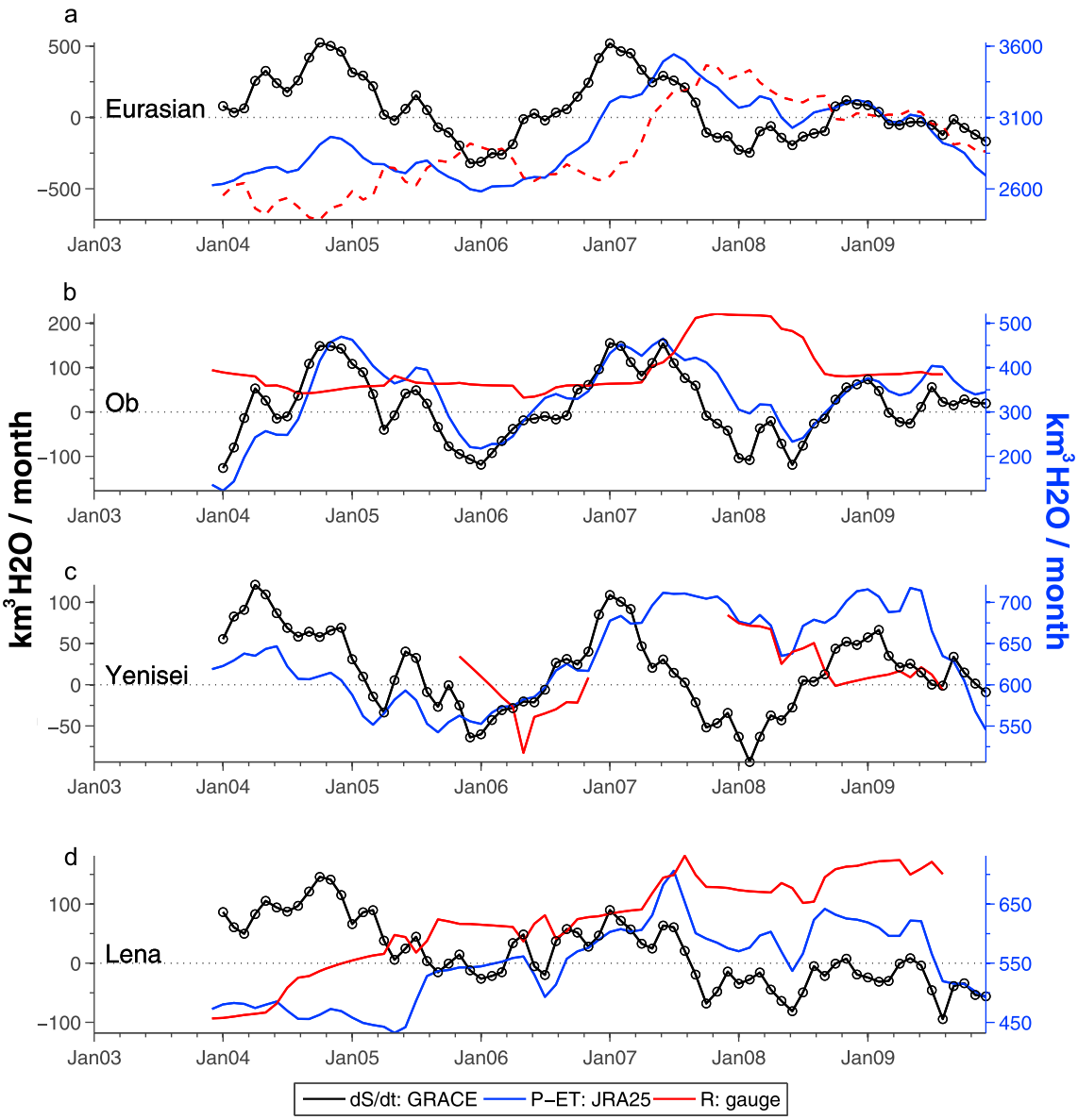

Figure 9. Annually accumulated fluxes for (a) pan-Arctic Eurasia, (b) Ob river basin, (c) Yenisei river basin, and (d) Lena river basin. At each time point, the values represent the integrated fluxes of the preceding 12 months; for example, the value for September 2008 is the sum of the monthly values between October 2007 and September 2008.

basin reflect the higher *R*/*P* ratios associated with regions of high permafrost coverage [*Serreze and Barry*, 2005]. From 2003 to 2007, P-ET into the basin has a similar positive slope and variability compared to gauged discharge over the same time period. Additionally, trends and variability in annually accumulated P-ET are very close to those of *P* from GPCP (not shown), consistent with the notion that P-ET variations tend to be highly correlated with variations in *P* [*Serreze and Barry*, 2005]. Following the peak in 2007, gauged discharge shows only a very modest increase, while annual P-ET markedly declines after the 2007 peak. This decrease in P-ET after 2007 is reflected in the negative TWS change rate inferred from GRACE (Figure 9). Between 2003 and 2007, the Lena basin was in a water accumulation mode, since then, the TWS in the basin has been declining, albeit at a slower rate than it was gaining in the accumulation period.

4. Discussion and Conclusion

[27] The terrestrial Eurasian Arctic regions have undergone significant changes over the last decades, as manifested in increasing annual river discharge, surface warming, and shifts in the seasonality of hydrologic variables [*Rawlins et al.*, 2009b]. Here, we have studied these changes from the perspective of terrestrial water storage variations. These direct, large-scale observations of TWS by GRACE are an essential contribution to understanding the driving mechanisms as well as the overall response of the terrestrial water cycle component in response to increasing discharge and precipi-

tation, in particular over the vast permafrost regions in the eastern parts of the drainage region.

[28] The attribution of increased discharge to the melting of excess ice in permafrost is not supported from GRACE measurements over the period 2003 to 2009. In all Eurasian basins draining into the Arctic Ocean, TWS has increased, albeit the trends are weak and interannual variations are strong. The combined in situ discharge from gauges over the three largest basins also shows tendencies of increase during this time, consistent with the long-term changes over the last 70 years (A. Shiklomanov, River discharge, in Arctic Report Card 2009, http://www.arctic.noaa.gov/reportcard). From the observed changes of TWS and discharge, it follows that net P-ET must have increased simultaneously in order to close the terrestrial hydrological budget. Our results thus lend further support to the hypothesis from *Rawlins et al.* [2009a] that net precipitation, in particular during the cold season, has increased and accounts for the observed discharge increase. Meltwater from excess permafrost ice, as proposed, e.g., by *Zhang et al.* [2005] and *Adam and Lettenmaier* [2008], does not need to be invoked to close the terrestrial water budget from 2003 to 2009. However, this does not mean that permafrost has not thawed. The observed increases of TWS, in particular over the Lena basin where discontinuous permafrost is present, suggest that more water is being retained in the subsurface through an increase of the active layer thickness, which is indicative of ongoing permafrost thaw. As outlined by *McClelland et al.* [2004], a thicker active layer may provide an indirect mechanism for increases in net P-ET through lowering the water table, thus limiting the terrestrial water available for evaporation and reducing the ET/*P* ratio. Additionally, warming soil temperatures and enhanced permeability of the soil are consistent with observed tendencies for increased winter snow precipitation over the Eurasian pan-Arctic drainage basins [*Rawlins et al.*, 2009a, 2009b], because the thicker snow layer prevents heat loss from the subsurface. Individual station observations of ground and soil temperatures in permafrost regions show a warming trend over the last decades [*Romanovsky et al.*, 2007], but significant decadal variations are also observed. While we do not know the full range of natural variability of TWS variations, GRACE observations clearly show that interannual variations in *dS*/*dt* have a similar magnitude compared to discharge and net precipitation variations. Thus, *dS*/*dt* needs to be taken into account for the terrestrial hydrological budget (equation (1)) and should not be assumed to be in equilibrium for time scales of at least 5–7 years, in particular during a time period where regime changes related to global warming are likely. Moreover, the increase of TWS over the permafrost regions indicates changing soil moisture and/or groundwater dynamics such that groundwater would play a more important role. Subsurface hydrology processes in turn have important ramifications for biogeochemical processes related to the storage and release of greenhouse gases [*Elberling et al.*, 2010]. In order to simulate these and to capture discharge trends, an advanced representation of subsurface storage dynamics including permafrost processes in hydrological models is necessary.

[29] As with any relatively short observational record of a climate process, the interpretation and attribution of apparent trends must be treated with care. Annual discharge over the study region shows pronounced interannual variability, making it very challenging to attribute any changes to recent global warming [*MacDonald et al.*, 2007]. In this context we note that the increases in net precipitation between 2003 and 2009 are not unprecedented compared to other 7 year periods in the JRA-25 data starting in 1979. Therefore, emerging trends could be related to interannual to decadal variability [*Serreze and Barry*, 2005]. The results of the present analysis underscore the need for continuous, long-term observations of all components of the terrestrial water budget in order to understand the controls and responses of high-latitude hydrology to global climate change.

[30] **Acknowledgments.** We acknowledge many productive conversations with D. Bromwich and M. Serreze. We thank three reviewers for their constructive comments that helped us to improve the paper and V. Zlotnicki and M. Watkins for support with the GRACE data and discussions. Permafrost data come from NSIDC (http://nsidc.org/data/ggd318.html [*Brown et al.*, 1998]), discharge observations come from the ArcticRIMS project (http://rims.unh.edu/data.shtml), and J. Alcamo and P. Döll are acknowledged for providing the WGHM model. F.W.L. was supported through the NASA Postdoctoral Program at Jet Propulsion Laboratory. This paper presents the results of one phase of research carried out at the Jet Propulsion Laboratory, California Institute of Technology, sponsored by the National Aeronautics and Space Administration (NASA).

References

Adam, J. C., and D. P. Lettenmaier (2008), Application of new precipitation and reconstructed streamflow products to streamflow trend attribution in Northern Eurasia, *J. Clim.*, *21*(8), 1807–1828.

Adam, J. C., I. Haddeland, F. Su, and D. P. Lettenmaier (2007), Simulation of reservoir influences on annual and seasonal streamflow changes for the Lena, Yenisei, and Ob rivers, *J. Geophys. Res.*, *112*, D24114, doi:10.1029/2007JD008525.

Adler, R. F., et al. (2003), The Version-2 Global Precipitation Climatology Project (GPCP) monthly precipitation analysis (1979–present), *J. Hydrometeorol.*, *4*(6), 1147–1167.

Alsdorf, D. E., and D. P. Lettenmaier (2003), Geophysics: Tracking fresh water from space, *Science*, *301*(5639), 1491–1494, doi:10.1126/science.1089802.

Berezovskaya, S., D. Yang, and D. L. Kane (2004), Compatibility analysis of precipitation and runoff trends over the large Siberian watersheds, *Geophys. Res. Lett.*, *31*, L21502, doi:10.1029/2004GL021277.

Brown, J., O. J. Ferrians, J. Heginbottom, and E. Melnikov (1998), Circum-Arctic map of permafrost and ground-ice conditions, February 2001 rev., http://nsidc.org/data/ggd318.html, Natl. Snow and Ice Data Cent., Boulder, Colo.

Chen, J. L., C. R. Wilson, J. S. Famiglietti, and M. Rodell (2007), Attenuation effect on seasonal basin-scale water storage changes from GRACE time-variable gravity, *J. Geod.*, *81*, 237–245, doi:10.1007/s00190-006-0104-2.

Cheng, M., and B. D. Tapley (2004), Variation's in the Earth's oblateness during the past 28 years, *J. Geophys. Res.*, *109*, B09402, doi:10.1029/2004JB003028.

Döll, P., and K. Fiedler (2008), Global-scale modeling of groundwater recharge, *Hydrol. Earth Syst. Sci.*, *12*(3), 863–885.

Döll, P., F. Kaspar, and B. Lehner (2003), A global hydrological model for deriving water availability indicators: Model tuning and validation, *J. Hydrol.*, *270*(1–2), 105–134, doi:10.1016/S0022-1694(02)00283-4.

Dommenget, D., and M. Latif (2002), A cautionary note on the interpretation of EOFs, *J. Clim.*, *15*(2), 216–225.

Duan, X., J. Guo, C. Shum, and W. van der Wal (2009), On the postprocessing removal of correlated errors in GRACE temporal gravity field solutions, *J. Geod.*, *83*, 1095–1106, doi:10.1007/s00190-009-0327-0.

Elberling, B., H. H. Christiansen, and B. U. Hansen (2010), High nitrous oxide production from thawing permafrost, *Nat. Geosci.*, *3*, 332–335.

Francis, J. A., D. M. White, J. J. Cassano, W. J. Gutowski, L. D. Hinzman, M. M. Holland, M. A. Steele, and C. J. Vörösmarty (2009), An Arctic hydrologic system in transition: Feedbacks and impacts on terrestrial, marine, and human life, *J. Geophys. Res.*, *114*, G04019, doi:10.1029/2008JG000902.

Güntner, A., J. Stuck, S. Werth, P. Doell, K. Verzano, and B. Merz (2007), A global analysis of temporal and spatial variations in continental water storage, *Water Resour. Res.*, *43*, W05416, doi:10.1029/2006WR005247.

Hannachi, A., I. T. Jolliffe, and D. B. Stephenson (2007), Empirical orthogonal functions and related techniques in atmospheric science: A review, *Int. J. Climatol.*, *27*(9), 1119–1152.

Held, I. M., and B. J. Soden (2006), Robust responses of the hydrological cycle to global warming, *J. Clim.*, *19*(21), 5686–5699.

Hirsch, R. M., and J. R. Slack (1984), A nonparametric trend test for seasonal data with serial dependence, *Water Resour. Res.*, *20*(6), 727–732, doi:10.1029/WR020i006p00727.

Klees, R., E. A. Zapreeva, H. C. Winsemius, and H. H. G. Savenije (2007), The bias in GRACE estimates of continental water storage variations, *Hydrol. Earth Syst. Sci.*, *11*, 1227–1241.

Koren, V., J. Schaake, K. Mitchell, Q. Duan, F. Chen, and J. Baker (1999), A parameterization of snowpack and frozen ground intended for NCEP weather and climate models, *J. Geophys. Res.*, *104*(D16), 19,569–19,585, doi:10.1029/1999JD900232.

Krokhin, V. V., and W. M. J. Luxemburg (2007), Temperatures and precipitation totals over the russian far east and eastern Siberia: Long-term variability and its links to teleconnection indices, *Hydrol. Earth Syst. Sci.*, *11*, 1831–1841.

MacDonald, G. M., K. V. Kremenetski, L. C. Smith, and H. G. Hidalgo (2007), Recent Eurasian river discharge to the Arctic Ocean in the context of longer-term dendrohydrological records, *J. Geophys. Res.*, *112*, G04S50, doi:10.1029/2006JG000333.

McClelland, J. W., R. M. Holmes, B. J. Peterson, and M. Stieglitz (2004), Increasing river discharge in the Eurasian Arctic: Consideration of dams, permafrost thaw, and fires as potential agents of change, *J. Geophys. Res.*, *109*, D18102, doi:10.1029/2004JD004583.

McClelland, J. W., S. J. Dery, B. J. Peterson, R. M. Holmes, and E. F. Wood (2006), A Pan-Arctic evaluation of changes in river discharge during the latter half of the 20th century, *Geophys. Res. Lett.*, *33*, L06715, doi:10.1029/2006GL025753.

Onogi, K., et al. (2007), The JRA-25 reanalysis, *J. Meteorol. Soc. Jpn.*, *85*(3), 369–432, doi:10.2151/jmsj.85.369.

Paulson, A., S. Zhong, and J. Wahr (2007), Inference of mantle viscosity from GRACE and relative sea level data, *Geophys. J. Int.*, *171*, 497–508, doi:10.1111/j.1365-246X.2007.03556.x.

Pavelsky, T. M., and L. C. Smith (2006), Intercomparison of four global precipitation data sets and their correlation with increased Eurasian river discharge to the Arctic Ocean, *J. Geophys. Res.*, *111*, D21112, doi:10.1029/2006JD007230.

Peterson, B. J., R. M. Holmes, J. W. McClelland, C. J. Vörösmarty, R. B. Lammers, A. I. Shiklomanov, I. A. Shiklomanov, and S. Rahmstorf (2002), Increasing river discharge to the Arctic Ocean, *Science*, *298*(5601), 2171–2173, doi:10.1126/science.1077445.

Peterson, B. J., J. McClelland, R. Curry, R. M. Holmes, J. E. Walsh, and K. Aagaard (2006), Trajectory shifts in the Arctic and subarctic freshwater cycle, *Science*, *313*(5790), 1061–1066, doi:10.1126/science.1122593.

Rawlins, M. A., M. C. Serreze, R. Schroeder, X. Zhang, and K. C. McDonald (2009a), Diagnosis of the record discharge of Arctic-draining Eurasian rivers in 2007, *Environ. Res. Lett.*, *4*(4), 045011, doi:10.1088/1748-9326/4/4/045011.

Rawlins, M. A., H. Ye, D. Yang, A. Shiklomanov, and K. C. McDonald (2009b), Divergence in seasonal hydrology across northern Eurasia: Emerging trends and water cycle linkages, *J. Geophys. Res.*, *114*(D18), D18119, doi:10.1029/2009JD011747.

Ray, R. D., and S. B. Luthcke (2006), Tide model errors and GRACE gravimetry: Towards a more realistic assessment, *Geophys. J. Int.*, *167*, 1055–1059.

Rodell, M., et al. (2004), The global land data assimilation system, *Bull. Am. Meteorol. Soc.*, *85*(3), 381–394.

Romanovsky, V., T. Sazonova, V. Balobaev, N. Shender, and D. Sergueev (2007), Past and recent changes in air and permafrost temperatures in eastern Siberia, *Global Planet. Change*, *56*(3–4), 399–413.

Rudolf, B., and U. Schneider (2004), Calculation of gridded precipitation data for the global land-surface using in-situ gauge observations, paper presented at 2nd Workshop of the International Precipitation Working Group IPWG, EUMETSAT, Darmstadt, Germany.

Schmidt, R., S. Petrovic, A. Güntner, F. Barthelmes, J. Wünsch, and J. Kusche (2008), Periodic components of water storage changes from GRACE and global hydrology models, *J. Geophys. Res.*, *113*, B08419, doi:10.1029/2007JB005363.

Serreze, M. C., and R. G. Barry (2005), *The Arctic Climate System*, 385 pp., Cambridge Univ. Press, Cambridge, U. K.

Serreze, M. C., and A. J. Etringer (2003), Precipitation characteristics of the Eurasian Arctic drainage system, *Int. J. Climatol.*, *23*(11), 1267–1291.

Serreze, M. C., and J. A. Francis (2006), The Arctic amplification debate, *Clim. Change*, *76*(3), 241–264.

Serreze, M. C., D. H. Bromwich, M. P. Clark, A. J. Etringer, T. Zhang, and R. Lammers (2002), Large-scale hydro-climatology of the terrestrial Arctic drainage system, *J. Geophys. Res.*, *107*(D2), 8160, doi:10.1029/2001JD000919.

Serreze, M. C., et al. (2006), The large-scale freshwater cycle of the Arctic, *J. Geophys. Res.*, *111*, C11010, doi:10.1029/2005JC003424.

Shiklomanov, A. I., and R. B. Lammers (2009), Record Russian river discharge in 2007 and the limits of analysis, *Environ. Res. Lett.*, *4*(4), 045015, doi:10.1088/1748-9326/4/4/045015.

Shiklomanov, A. I., R. B. Lammers, M. A. Rawlins, L. C. Smith, and T. M. Pavelsky (2007), Temporal and spatial variations in maximum river discharge from a new Russian data set, *J. Geophys. Res.*, *112*, G04S53, doi:10.1029/2006JG000352.

Slater, A. G., T. J. Bohn, J. L. McCreight, M. C. Serreze, and D. P. Lettenmaier (2007), A multimodel simulation of Pan-Arctic hydrology, *J. Geophys. Res.*, *112*, G04S45, doi:10.1029/2006JG000303.

Smith, L. C., Y. Sheng, G. M. MacDonald, and L. D. Hinzman (2005), Disappearing Arctic lakes, *Science*, *308*(5727), 1429, doi:10.1126/science.1108142.

Smith, L. C., T. M. Pavelsky, G. M. MacDonald, A. I. Shiklomanov, and R. B. Lammers (2007), Rising minimum daily flows in northern Eurasian rivers: A growing influence of groundwater in the high-latitude hydrologic cycle, *J. Geophys. Res.*, *112*, G04S47, doi:10.1029/2006JG000327.

Solomon, S., et al. (2007), Technical summary, in *Climate Change* 2007*: The Physical Science Basis. Contribution of Working Group I to the Fourth Assessment Report of the Intergovernmental Panel on Climate Change*, edited by S. Solomon et al., pp. 20–91, Cambridge Univ. Press, Cambridge, U. K.

Stroeve, J., M. M. Holland, W. Meier, T. Scambos, and M. Serreze (2007), Arctic sea ice decline: Faster than forecast, *Geophys. Res. Lett.*, *34*(9), L09501, doi:10.1029/2007GL029703.

Swenson, S., and J. Wahr (2002), Methods for inferring regional surface-mass anomalies from Gravity Recovery and Climate Experiment (GRACE) measurements of time-variable gravity, *J. Geophys. Res.*, *107*(B9), 2193, doi:10.1029/2001JB000576.

Swenson, S., and J. Wahr (2003), Monitoring changes in continental water storage with GRACE, *Space Sci. Rev.*, *108*, 345–354, doi:10.1023/A:1026135627671.

Swenson, S., and J. Wahr (2006a), Estimating large-scale precipitation minus evapotranspiration from GRACE satellite gravity measurements, *J. Hydrometeorol.*, *7*(2), 252–270, doi:10.1175/JHM478.1.

Swenson, S., and J. Wahr (2006b), Post-processing removal of correlated errors in GRACE data, *Geophys. Res. Lett.*, *33*, L08402, doi:10.1029/2005GL025285.

Swenson, S., D. Chambers, and J. Wahr (2008), Estimating geocenter variations from a combination of GRACE and ocean model output, *J. Geophys. Res.*, *113*, B08410, doi:10.1029/2007JB005338.

Syed, T. H., J. S. Famiglietti, V. Zlotnicki, and M. Rodell (2007), Contemporary estimates of pan-arctic freshwater discharge from GRACE and reanalysis, *Geophys. Res. Lett.*, *34*, L19404, doi:10.1029/2007GL031254.

Tapley, B. D., S. Bettadpur, J. R. Ries, P. F. Thompson, and M. M. Watkins (2004), GRACE measurements of mass variability in the Earth systems, *Science*, *305*(5683), 503–505, doi:10.1126/science.1099192.

Taylor, K. E. (2001), Summarizing multiple aspects of model performance in a single diagram, *J. Geophys. Res.*, *106*(D7), 7183–7192, doi:10.1029/2000JD900719.

Vörösmarty, C. J., B. M. Fekete, M. Meybeck, and R. B. Lammers (2000), Geomorphometric attributes of the global system of rivers at 30-minute spatial resolution, *J. Hydrol.*, *237*(1–2), 17–39, doi:10.1016/S0022-1694(00)00282-1.

Wahr, J., M. Molenaar, and F. Bryan (1998), Time variability of the Earth's gravity field: Hydrological and oceanic effects and their possible detection using GRACE, *J. Geophys. Res.*, *103*(B12), 30,205–30,229, doi:10.1029/98JB02844.

Wahr, J., S. Swenson, and I. Velicogna (2006), Accuracy of GRACE mass estimates, *Geophys. Res. Lett.*, *33*, L06401, doi:10.1029/2005GL025305.

Werth, S., and A. Güntner (2010), Calibration analysis for water storage variability of the global hydrological model WHGM, *Hydrol. Earth Syst. Sci.*, *14*(1), 59–78.

Zhang, T., et al. (2005), Spatial and temporal variability in active layer thickness over the Russian Arctic drainage basin, *J. Geophys. Res.*, *110*, D16101, doi:10.1029/2004JD005642.

J. O. Dickey and F. W. Landerer, Jet Propulsion Laboratory, California Institute of Technology, 4800 Oak Grove Dr., MS 238-600, Pasadena, CA 91109, USA. (landerer@jpl.nasa.gov)

A. Güntner, Helmholtz Centre Potsdam, GFZ German Research Centre for Geosciences, D-14473 Potsdam, Germany.